

Egyptian Journal of Chemistry

http://ejchem.journals.ekb.eg/



Synergistic synthesis: Optimizing natural alginate/carrageenan polysaccharides crosslinked with polyacrylic acid for enhanced Rhodamine B removal in aqueous environments



Chiraz Ammar 1, Ghadah A. Alharbi 2, Yassine El-Ghoul 2*

¹ Department of Fashion Design, College of Arts and Design, Qassim University, Buraidah 51452, Saudi Arabia; ² Department of Chemistry, College of Science, Qassim University, Buraidah 51452, Saudi Arabia;

Abstract

The discharge of synthetic dyes into aquatic systems poses a persistent environmental and health threat due to their stability, toxicity, and resistance to biodegradation. Rhodamine B dye (RhB), a widely used cationic dye, is particularly problematic and demands effective remediation strategies. In this work, a novel crosslinked ternary composite adsorbent based on alginate, poly(acrylic acid), and λ -carrageenan (poly-AG/PAA/ λ -CAR) was synthesized and evaluated for RhB removal. The composite structure and morphology were confirmed by Fourier-transform infrared spectroscopy (FTIR), swelling studies, and scanning electron microscopy (SEM). Batch adsorption experiments demonstrated that removal efficiency was strongly influenced by pH, initial concentration, contact time, and adsorbent dosage. Optimal RhB removal occurred at pH 8, reaching equilibrium within 60 min. Adsorption followed the PSO model (R² > 0.99), indicating chemisorption. The Langmuir model fitted best, with a maximum capacity of 1111.1 mg g⁻¹ (R² = 0.99), while the Freundlich model suggested multilayer adsorption on a heterogeneous surface. The Temkin isotherm further highlighted robust adsorbate, adsorbent interactions, with a binding energy of 42.51 kJ mol⁻¹. The outstanding performance of the poly-AG/PAA/ λ -CAR composite is attributed to the synergistic contributions of alginate's carboxyl groups, λ -carrageenan's sulfate functionalities, and the structural resilience of poly(acrylic acid). These findings establish poly-AG/PAA/ λ -CAR as a sustainable, efficient, and reusable adsorbent for cationic dye removal, offering a promising alternative for the treatment of industrial wastewater.

Keywords: Polymer; alginate; carrageenan; SEM; adsorption; isotherms; dye environmental application.

1. Introduction

The rapid growth of industrial activities has led to the widespread use of synthetic dyes in textiles, cosmetics, papermaking, and printing. Due to their complex aromatic structures, these dyes are highly resistant to biological degradation, making them persistent pollutants once discharged into aquatic environments. Their release not only deteriorates water quality but also poses serious risks to ecosystems and human health [1-4]. Consequently, the removal of dyes from wastewater remains a critical challenge for environmental protection and public safety.

Conventional treatment technologies, such as chemical precipitation [5], ion exchange [6], membrane filtration [7], and electrochemical recovery, have been extensively employed for the removal of contaminants, particularly pollutant dyes. However, each of these methods has notable limitations. Chemical precipitation is efficient only at high concentrations (>100 ppm) and generates large volumes of hazardous sludge requiring costly disposal [8]. Ion exchange processes suffer from resin fouling, competitive ion effects, and elevated operational costs [9]. Membrane-based processes such as nanofiltration and reverse osmosis achieve excellent rejection rates, but are constrained by high energy demand and membrane scaling [10]. Electrochemical techniques, while effective, demand sophisticated infrastructure and uninterrupted power supply. These drawbacks have intensified research efforts toward alternative solutions, with adsorption emerging as one of the most promising techniques for wastewater remediation due to its simplicity, cost-effectiveness, versatility, and high efficiency [11] The performance of adsorption depends strongly on the physicochemical properties of the adsorbent, including surface area, pore structure, and the availability of active functional groups [12,13]. In this regard, biopolymer-based adsorbents have gained considerable attention owing to their natural abundance, biocompatibility, and inherent functional groups that promote pollutant binding. Polysaccharides such as alginate, carrageenan, and chitosan are particularly attractive because they are renewable, biological, biodegradable properties, and rich in reactive groups [14-20]. Alginate, derived from brown algae, contains guluronic acid blocks capable of coordinating divalent cations through the classical "egg-box" model [21]. Carrageenans, especially λ -carrageenan extracted from red seaweed, exhibit high sulfate group density ($-OSO_3$), enabling

*Corresponding author e-mail: <u>y.elghoul@qu.edu.sa</u>.; (Yassine El-Ghoul).

Received Date: 20 September 2025, Revised Date: 18 October 2025, Accepted Date: 11 November 2025

DOI: 10.21608/EJCHEM.2025.425544.12362

©2026 National Information and Documentation Center (NIDOC)

strong electrostatic interactions with cationic pollutants [22]. However, while these natural polymers offer strong adsorption affinity, their mechanical strength and stability are often limited.

To overcome these shortcomings, synthetic polymers such as poly(acrylic acid) (PAA) are increasingly incorporated to form hybrid networks. PAA contributes abundant carboxyl groups (-COOH) that serve as additional coordination sites for dye molecules, while also improving the structural robustness of the composite material [23,24]. Such functionalization strategies not only enhance adsorption performance but also broaden the applicability of these materials to a range of pollutants. Previous studies have demonstrated the benefits of binary composites; for instance, alginate-polyacrylamide hydrogels exhibited improved methylene blue uptake compared with pure alginate [25], while carrageenan/chitosan composites showed high removal efficiency for both anionic and cationic dyes [26]. Despite these advances, there remains a notable gap in the development of ternary composite systems that strategically combine alginate, PAA, and λ -carrageenan to exploit their complementary functionalities.

In this work, we address this research gap by designing and synthesizing a novel ternary composite adsorbent, alginate/poly(acrylic acid)/ λ -carrageenan (poly-AG/PAA/ λ -CAR). This material integrates three key features including the carboxyl-rich structure of PAA for enhanced dye coordination, the gel-forming ability of alginate for structural stability, and the high sulfate content of λ -carrageenan for improved electrostatic and hydrogen-bonding interactions. We hypothesize that the synergy of these components will yield superior adsorption performance compared with existing biopolymer-based adsorbents, with improvements in reusability, selectivity, and overall dye uptake.

To test this hypothesis, we evaluated the adsorption of Rhodamine B (RdB), a representative cationic dye and priority pollutant, under varying pH, concentration, and temperature conditions. The adsorption mechanisms were further investigated through kinetic and isotherm modeling. The structural and physicochemical properties of the composite were characterized by Fourier-transform infrared spectroscopy (FTIR), swelling studies, and scanning electron microscopy (SEM). The findings of this study not only provide a sustainable and efficient material for dye removal but also contribute to advancing the design of polysaccharide-based hybrid adsorbents for environmental remediation.

2. Materials and Methods

2.1 Materials

Rhodamine B dye ($C_2 \otimes H_3 \cap CIN_2 \otimes G_3$, AR grade, 99%), sodium alginate (AG; degree of deacetylation \approx 70%, medium viscosity, Mw \approx 30,000 g/mol), poly(acrylic acid) (PAA; Mw \approx 1800 g/mol), and λ -carrageenan (CAR; Mw \approx 446 kDa, fine white powder) were purchased from Sigma-Aldrich (St. Louis, MO, USA). All reagents were of analytical grade and were used as received without further purification.

2.2. Characterization of the polymers

The structural and morphological properties of the poly-AG/PAA/ λ -CAR composite and its constituent biopolymers were thoroughly characterized using FTIR spectroscopy, scanning electron microscopy (SEM), and swelling analysis.

2.2.1. Fourier-Transform Infrared (FTIR) Spectroscopy

FTIR spectra were acquired using a Gladi-ATR spectrophotometer (Agilent Technologies, Santa Clara, CA, USA) equipped with an attenuated total reflection (ATR) accessory. A background spectrum was recorded prior to measurements to correct for atmospheric interference. Spectra were collected over the range of 4000-400 cm⁻¹ with a resolution of 4 cm⁻¹, averaging 32 scans per sample to ensure high signal-to-noise ratio and reproducibility. This analysis allowed identification of functional groups and confirmation of crosslinking within the hydrogel network.

2.2.2. Scanning Electron Microscopy (SEM)

The surface morphology of the composite and individual biopolymers was examined using a scanning electron microscope (model/manufacturer). Samples were dried, mounted on aluminum stubs with double-sided conductive carbon tape, and sputter-coated with a thin layer of gold to enhance conductivity. SEM micrographs captured at various magnifications provided insights into the surface texture, porosity, and overall structural features, which are critical for understanding adsorption behavior.

2.2.3. Swelling Behavior

The water uptake capacity was determined using a gravimetric method. The dry mass of each sample (m_i) was measured after complete drying. Samples were immersed in distilled water for up to 48 hours, and at predetermined intervals, removed, gently blotted to remove surface moisture, and weighed to determine the hydrated mass (mf). The swelling ratio (SR%) was calculated using the following equation:

%-SR=
$$((mf-mi))/mi \times 100$$
 (1)

This approach allowed the evaluation of water absorption kinetics, providing quantitative information on the hydrophilic character and crosslinked network architecture of the materials. 2.3. Preparation of Metal Solutions

Analytical-grade metal salts (Sigma-Aldrich) were dissolved in deionized water to produce stock solutions (1000 mg L^{-1}) of chromium (Cr), cobalt (Co), and nickel (Ni). Serial dilution was employed to produce working solutions ranging from 5 to 500 mg/L. The pH of each solution was calibrated using a calibrated pH meter (Model XYZ, accuracy ± 0.01) and monitored using 0.1 M NaOH or HCl to adjust the pH.

2.4. Batch Biosorption Studies

Batch adsorption experiments were performed to investigate the removal of Rhodamine B (RhB) using the poly-AG/PAA/λ-CAR composite. Stock solutions of RhB were prepared by dissolving the dye in distilled water, and working solutions of desired concentrations were obtained by dilution immediately before use. Known volumes of RhB solution were transferred into 100 mL conical flasks, and a specified amount of the adsorbent was added. The suspensions were agitated continuously at 150 rpm on a mechanical shaker to ensure uniform interaction between the dye molecules and the adsorbent.

The influence of various parameters on adsorption efficiency was systematically evaluated, including contact time, initial dye concentration, adsorbent dosage, solution pH, and temperature. Contact time studies were conducted by sampling at specific intervals until equilibrium was achieved (from 0 to 120 min). Adsorbent dosage was varied from 0 to 800 mg/L to determine the optimum amount for maximum RhB removal. The pH of the dye solutions was adjusted using 0.1 M HCl or 0.1 M NaOH to evaluate the effect of pH on the adsorption (pH varied from 2 to 12). Temperature-dependent experiments were performed at 22, 40, and 60 °C to assess the effect of thermal conditions on adsorption via three isotherms.

After each experiment, the adsorbent was separated by filtration, and the residual RhB concentration in the solution was determined using a UV-Vis spectrophotometer at 554 nm. The adsorption capacity at equilibrium and the percentage of dye removal were calculated to assess performance. All experiments were conducted in triplicate, and the average values were reported.

2.5 Data Analysis

2.5.1 Adsorption performance evaluation

The efficiency of dye removal, adsorption capacity, and the corresponding isotherm and kinetic parameters were calculated using the following expressions:

Removal Efficiency:
$$R (\%) = (\text{Co-Ct})/\text{Co} \times 100$$
 (2)

where R(%) represents the percentage removal of dye, C₀ (mg/L) is the initial dye concentration, and C (mg/L) is the concentration at time t.

Adsorption Capacity:
$$qt = (\text{Co-Ct})/\text{m} \times \text{V}$$
 (3)
 $qe = (\text{Ce})/\text{m} \times \text{V}$ (4)

where q (mg/g) and $q_e(mg/g)$ denote the adsorption capacities at time t and at equilibrium, respectively; $C_e(mg/L)$ is the equilibrium dye concentration, V (L) is the volume of the solution, and m (g) is the adsorbent mass.

2.5.2 Adsorption Isotherms:

The equilibrium adsorption data were analyzed using both the Langmuir and Freundlich models.

Langmuir isotherm (monolayer adsorption on a uniform surface):

$$C_e/Q_e = 1/(Q_max K_L) + C_e/Q_max$$
 (5)

Freundlich isotherm (multilayer adsorption on a heterogeneous surface):

$$Log Q_e = log K_f + 1/n Log C_e$$
 (6)

Here, Q ax (mg g⁻¹) is the maximum adsorption capacity, K^L (L mg⁻¹) is the Langmuir constant, K^f is the Freundlich adsorption capacity factor, and 1/n represents the adsorption intensity.

The Langmuir model assumes adsorption occurs at specific homogeneous sites, forming a single molecular layer, whereas the Freundlich model accounts for surface heterogeneity and the possibility of multilayer adsorption.

2.5.3 Adsorption Kinetics:

The kinetics of adsorption were examined using pseudo-first-order (PFO) and pseudo-second-order (PSO) models. Pseudo-first-order model (PFO):

$$Log (qe-qt) = log qe - k_1t$$
 (7)

Pseudo-second-order (PSO):

$$t/qt = 1/k_2qe^2 + t/qe$$
 (8)

In these expressions, k_1 (min⁻¹) and k_2 (g mg⁻¹ min⁻¹) are the rate constants of the respective models. Model fitting was carried out using linear least-squares regression to assess the applicability of each kinetic model.

3. Results and discussion

3.1. Preparation of the crosslinked polymer

Alginate and λ-carrageenan biopolymers were crosslinked with poly(acrylic acid) at a compositional ratio of 3:2:3 (AG/PAA/CAR), resulting in the formation of the poly(AG/PAA/λ-CAR) polymer composite. Crosslinking was achieved through a polyesterification reaction in which the carboxyl groups of PAA interacted with the hydroxyl functionalities of the glycosidic backbones of alginate and carrageenan. This dual interaction facilitated the construction of a robust threedimensional polymeric network, where both natural polysaccharides were covalently anchored to the PAA polymer via ester

The formation of these covalent bridges not only enhanced the mechanical stability and structural integrity of the hydrogel but also improved its adsorption capacity. The coexistence of hydroxyl, carboxyl, and ester groups within the network provided abundant active binding sites, thereby promoting efficient interaction with cationic dye molecules.

3.2. Infrared analysis

Fourier-transform infrared (FT-IR) analysis was carried out to confirm the successful formation of the poly-AG/PAA/λ-CAR network and to elucidate its characteristic functional groups. The obtained spectrum (Figure 1) displayed a distinct absorption band at 1735 cm⁻¹, corresponding to the stretching vibrations of ester carbonyl groups. This feature provides clear evidence of ester bond formation, resulting from the reaction between the carboxylic functionalities of PAA and the hydroxyl groups present in alginate and carrageenan. In addition, a broad signal around 3431 cm⁻¹ was assigned to O–H stretching, while a peak near 1035 cm⁻¹ was related to C–O–C stretching vibrations of the glycosidic backbone. Absorptions between 1000 and 1100 cm⁻¹ further indicated the presence of pyranose ring vibrations [27]. Distinctive bands characteristic of carrageenan sulfate groups were also recorded at 1215, 922, and 833 cm⁻¹ [28,29]. Collectively, these spectral features confirm the integration of hydroxyl, carboxyl, ester, and sulfate moieties within the polymer matrix, which are essential for providing active binding sites in adsorption applications.

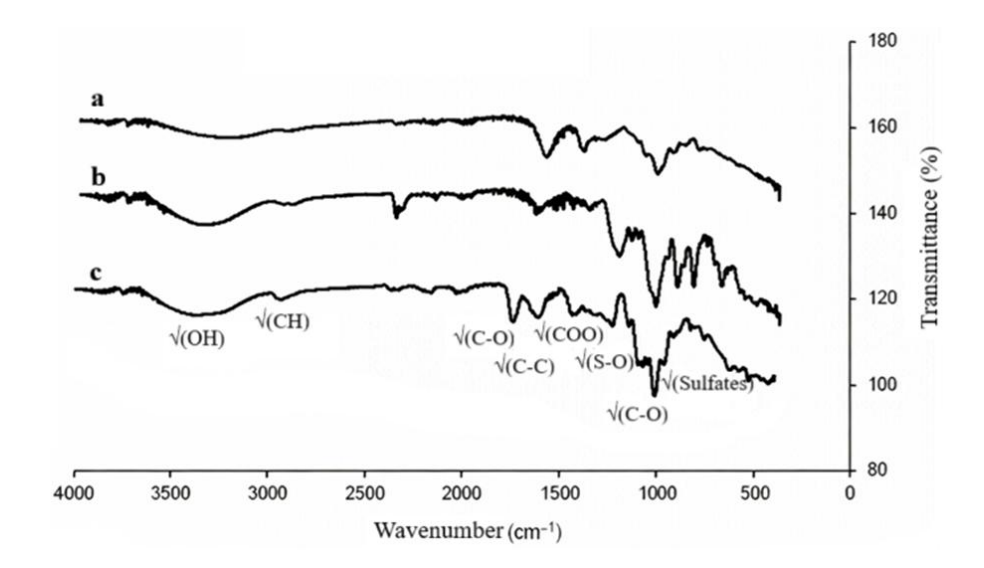


Figure 1. FT-IR spectra of the alginate (a), carrageenan (b) and the crosslinked poly-AG/PAA/λ-CAR biopolymer (c).

3.2. Swelling behavior

The swelling characteristics of the polymeric samples were examined as a function of impregnation time, and the outcomes for alginate (AG) and carrageenan (CAR) are shown in Figure 2. Both polymers approached a pseudo-equilibrium after nearly 5 hours, at which point maximum swelling ratios of 191% and 248% were recorded for AG and CAR, respectively. A gradual increase in swelling ratio was observed with increasing immersion time for all tested systems. Remarkably, the crosslinked poly-AG/PAA/ λ -CAR network exhibited a swelling capacity more than double that of the individual uncrosslinked polymers, highlighting its superior hydrophilic behavior. This enhanced performance is ascribed to the combined water-attracting properties of carrageenan and alginate, reinforced by the presence of poly(acrylic acid) (PAA) as a crosslinker, all of which are well recognized for their strong hydrophilicity [30,31].

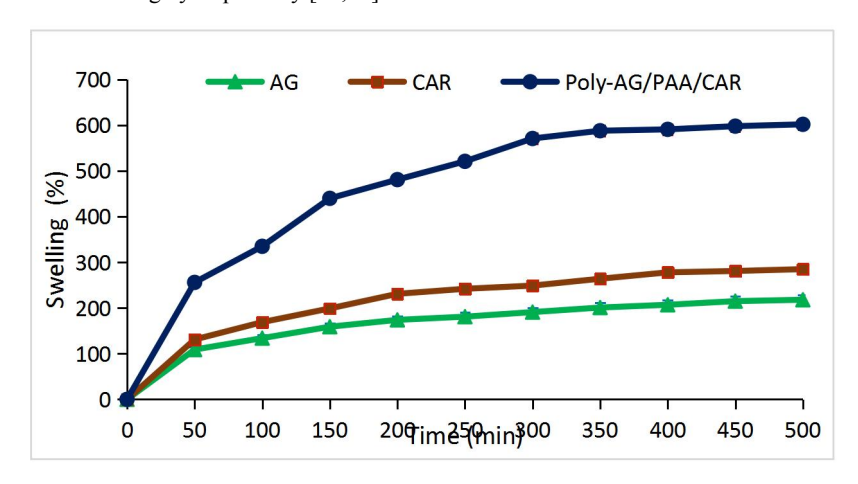


Figure 2. Swelling behavior of alginate (AG), carrageenan (CAR), and the crosslinked poly-AG/PAA/λ-CAR polymers over different impregnation times.

Egypt. J. Chem. 69, No. 2 (2026)

The crosslinked biopolymer network exhibited enhanced hydrophilicity, which increased water uptake and facilitated more effective diffusion and binding of dye molecules to the polymer's active sites.

3.3. SEM analysis

The SEM images of the crosslinked poly-AG/PAA/λ-CAR polymer (Figure 3) reveal a markedly rougher and more porous surface compared to the native alginate and carrageenan biopolymers. This morphological change results from the esterification reaction with PAA polymer, which not only chemically crosslinks the polymer chains but also generates a more open and irregular surface structure.

The increased porosity and surface roughness suggest enhanced hydrophilicity, facilitating greater water penetration and diffusion into the polymer network [32-33]. The interconnected pore structure exposes internal functional groups, such as hydroxyl, carboxyl, ester, and sulfate moieties, that are critical for dye adsorption.

Such a surface morphology benefits dye removal by enabling faster diffusion of dye molecules into the polymer matrix, increasing the contact area, and promoting more effective utilization of adsorption sites. Overall, the SEM observations confirm successful structural modification of the biopolymer network and support the improved adsorption efficiency of the modified polymer system.

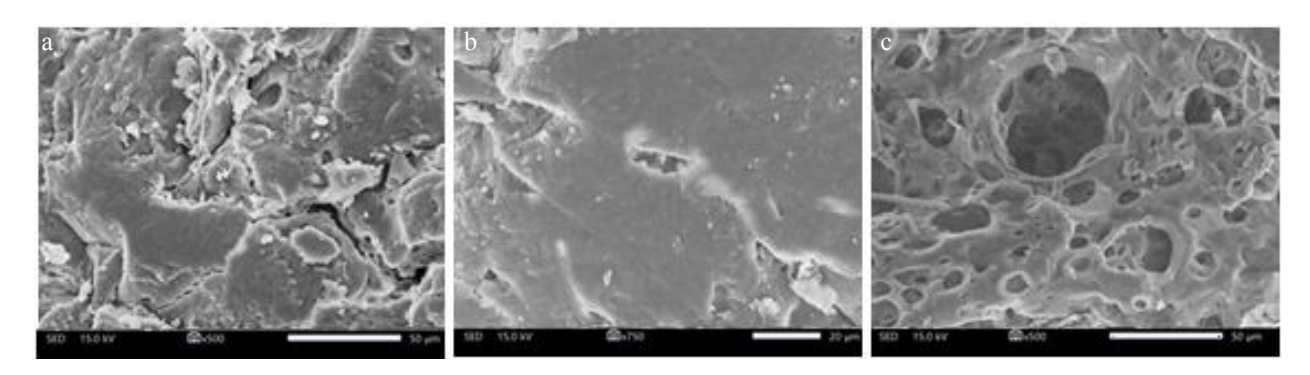


Figure 3. SEM mimeographs of the alginate (a), carrageenan (b) and the crosslinked poly-AG/PAA/λ-CAR biopolymer (c).

3.1 Batch adsorption experiments

3.1.1 pH-responsive adsorption characteristics

The pH of the dye solution is a key parameter governing the adsorption of Rhodamine B (RhB) onto the poly-AG/PAA/λ-CAR composite. As illustrated in Figure 4, the maximum removal efficiency was achieved at pH 8. RhB is a cationic dye that dissociates into positively charged ions in aqueous solution. At lower pH values (acidic medium), the carboxyl and sulfate groups present in alginate, carrageenan, and poly(acrylic acid) remain largely protonated, resulting in reduced negative charge density on the adsorbent surface. Nevertheless, moderate adsorption still occurs through hydrogen bonding and weak electrostatic interactions. As the pH increases, deprotonation of carboxyl and sulfate groups takes place, leading to an increase in negative surface charge. This enhances the electrostatic attraction between the negatively charged polymeric network and the positively charged RhB molecules, thereby improving adsorption efficiency. The maximum adsorption at pH 8 indicates an optimal balance where the polymer surface is sufficiently deprotonated to promote strong electrostatic attraction, while dye molecules remain cationic and readily available for binding. Beyond pH 8, in strongly alkaline media, the adsorbent surface acquires an excess of negative charges, but competitive interactions with hydroxide ions (OH-) and changes in RhB speciation reduce the effective binding. In addition, partial aggregation of dye molecules at higher pH may limit accessibility to active sites. As a result, adsorption capacity stabilizes and does not increase further [34].

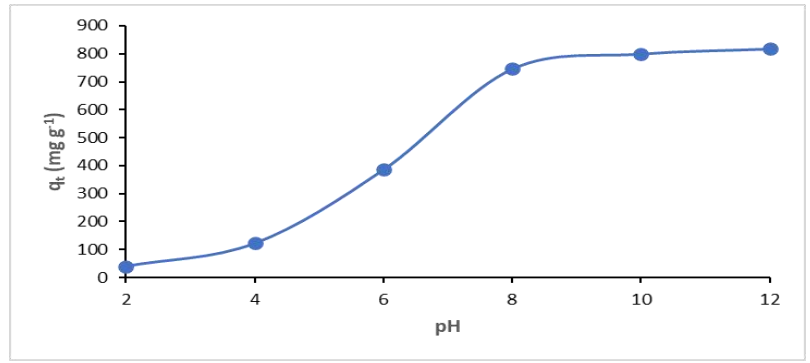


Figure 4. Effect of pH on RhB adsorption onto the poly-AG/PAA/λ-CAR polymeric composite

3.1.2 Dose-Dependent Adsorption Behavior

its effectiveness as a promising bio-sorbent system.

The adsorption of RhB cationic dye onto the poly-AG/PAA/λ-CAR composite was examined across a range of initial dye concentrations (50-1000 mg L⁻¹) under optimized conditions (pH 8, temperature 22 °C, and contact time 120 min). As illustrated in Figure 5, the adsorption capacity increased steadily with rising dye concentration. At the highest tested concentration (1000 mg L^{-1}), the composite exhibited a maximum removal capacity of 764.5 mg g^{-1} , which is a remarkable result. This enhanced performance can be attributed to the pronounced hydrophilic nature of the crosslinked network, as previously evidenced by the swelling studies. The abundance of hydroxyl groups from alginate and carrageenan, combined with the carboxylic groups of PAA, provided abundant binding sites for dye uptake. At around 500 mg L⁻¹, the adsorption curve tended to level off, forming a pseudo-plateau that reflects near-saturation of available sites. Compared with other reported polymeric adsorbents, the poly-AG/PAA/λ-CAR composite demonstrated superior dye uptake capacity, confirming

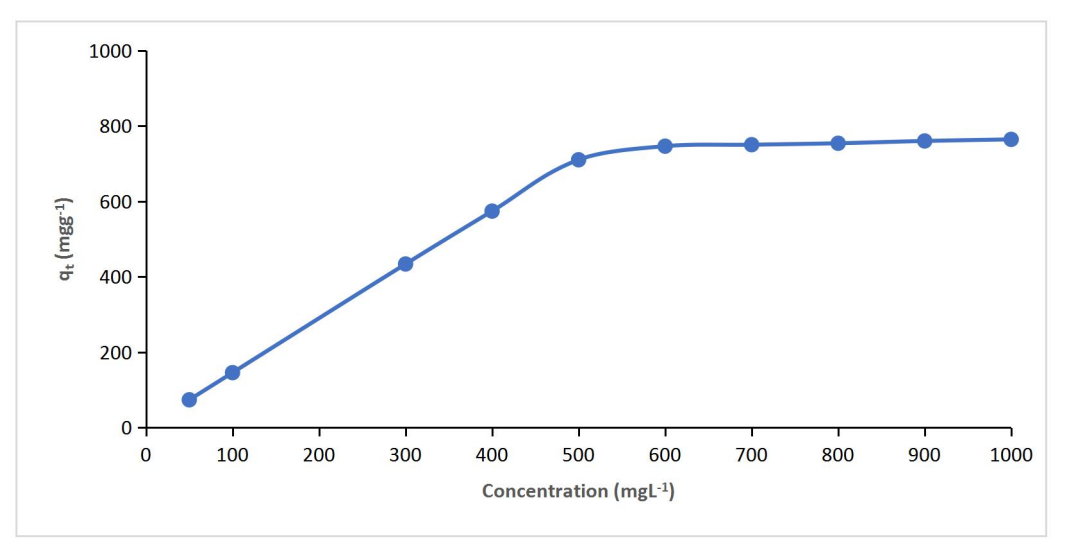


Figure 5. Effect of adsorbent dosage on RhB removal efficiency using the poly-AG/PAA/λ-CAR composite.

3.1.3 Time-Dependent Adsorption Kinetics

Equilibrium was reached after approximately 120 min (Figure 6). The adsorption process was rapid in the initial stage (0-50 min), during which more than 80% of the dye was removed. This fast uptake can be attributed to the abundance of readily accessible active sites on the adsorbent surface. Beyond this period, the adsorption gradually leveled off, indicating the progressive saturation of available sites and the establishment of equilibrium. The maximum adsorption capacity for methylene blue was determined to be 746.5 mg/g. This remarkably high sorption performance is likely due to the presence of additional functional groups, such as carboxylate and sulfonate moieties, introduced through the poly-AG/PAA/λ-CAR composite

Within 60 minutes, the adsorption process achieved near-equilibrium, resulting in 98% dye removal.

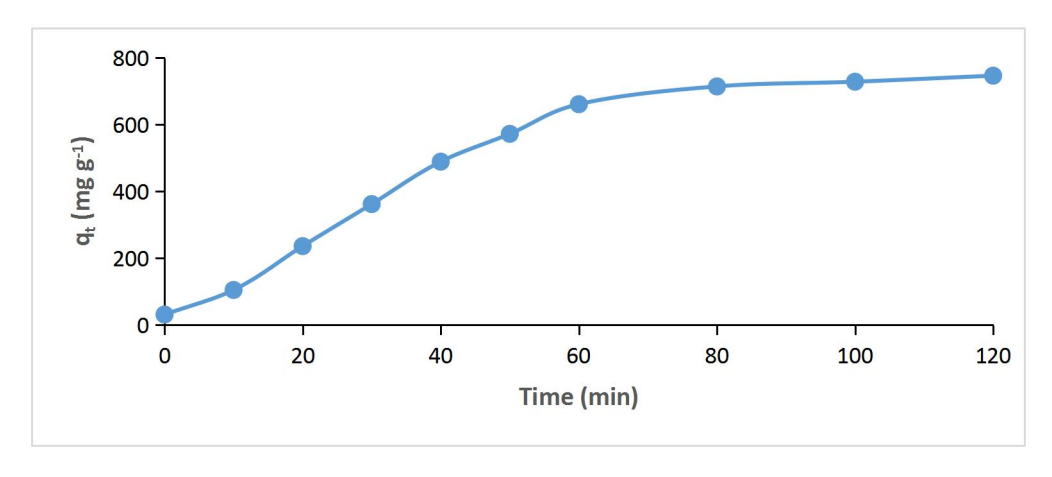


Figure 6. Kinetic study of RhB adsorption onto the poly-AG/PAA/λ-CAR composite.

Egypt. J. Chem. 69, No. 2 (2026)

The rapid equilibration of the composite is attributed to the complete saturation of its active sites, as reflected by the plateau in removal efficiency sustained after 60 minutes. The adsorption kinetics reveal a biphasic pattern, consisting of an initial rapid surface adsorption phase (0-40 minutes) followed by a slower intraparticle diffusion phase (40-60 minutes). This two-step behavior is characteristic of polysaccharide-based adsorbents [35] and highlights the synergistic interaction between the alginate, carrageenan, and polyacrylic acid components.

3.1.4 Effect of temperature on the adsorption of RhB dye

The experimental data (Figure 7) demonstrate that the adsorption efficiency of the poly-AG/PAA/λ-CAR composite is moderately affected by temperature. Temperature is a critical factor in adsorption performance, primarily influencing two aspects: the swelling behavior of the adsorbent and the thermodynamic nature (exothermic or endothermic) of the adsorption process at equilibrium. For a dye concentration of 600 mg L⁻¹ and a contact time of 120 min, the adsorption capacity was evaluated at 22, 40, and 60 °C. The results exhibited a consistent trend across all tested temperatures, with adsorption performance decreasing gradually as temperature increased. This decline indicates that the interaction between the poly-AG/PAA/λ-CAR adsorbent and the reactive anionic dye is exothermic in nature. The reduction in adsorption capacity at higher temperatures can be attributed to the partial reversibility of the adsorption mechanism and the unfavorable influence of thermal energy on the adsorbent-dye interactions. [36].

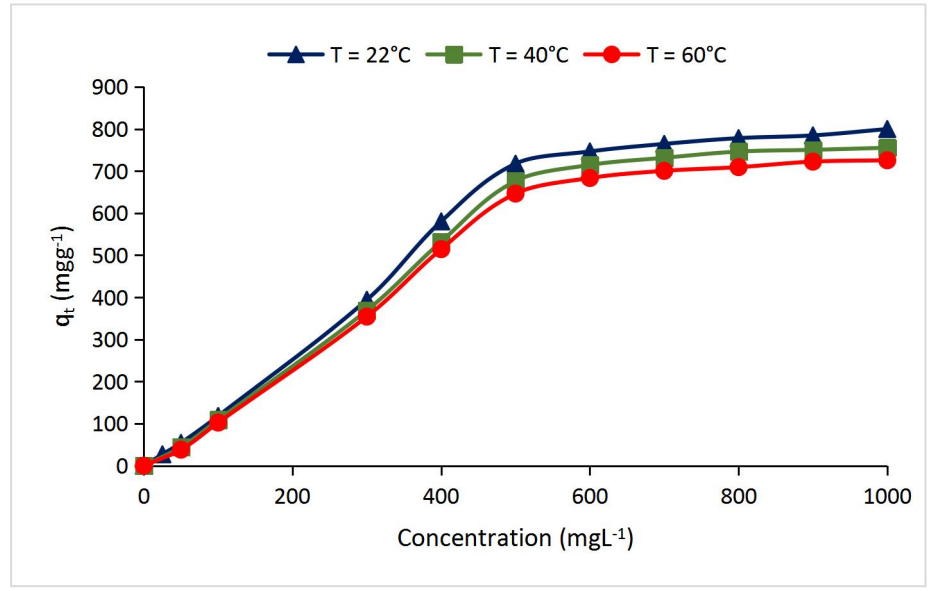


Figure 7. Adsorption capacity of the poly-AG/PAA/\(\lambda\)-CAR composite as a function of temperature.

3.2 Adsorption Kinetics

The adsorption behavior of RhB cationic dye on the synthesized poly-AG/PAA/λ-CAR composite was analyzed using different kinetic models, namely the pseudo-first-order (Figure 8a), pseudo-second-order (Figure 8b), Elovich (Figure 8c), and intra-particle diffusion models (Figure 8d). The kinetic constants for each model were obtained from the corresponding linear plots, and the calculated parameters are summarized in Table 1.

The pseudo-first-order model exhibited relatively low correlation coefficients (R² values between 0.80 and 0.83), suggesting that this model is inadequate for describing the adsorption kinetics of RhB under the present conditions. Similar to earlier studies, such discrepancies are often attributed to the fact that the pseudo-first-order equation is generally valid only during the initial adsorption stage and fails to describe the overall kinetic process [37].

In contrast, the pseudo-second-order model provided an excellent fit, with correlation coefficients (R2) consistently greater than 0.99. This high level of agreement implies that the adsorption process was predominantly controlled by chemisorption, involving valence forces through electron sharing or exchange between the adsorbent surface and RhB molecules [38].

The Elovich model (Figure 8c) also gave a satisfactory fit, suggesting that surface heterogeneity and activation energies may contribute to the adsorption process. However, its correlation coefficients were still slightly lower than those of the pseudosecond-order model, confirming that chemisorption was the dominant mechanism.

Finally, the intra-particle diffusion model (Figure 8d) exhibited linearity with the regression line passing through the origin. This suggests that intra-particle diffusion was the sole rate-limiting step, indicating that the adsorption process was predominantly governed by pore diffusion without significant influence from external mass transfer or surface adsorption [39].

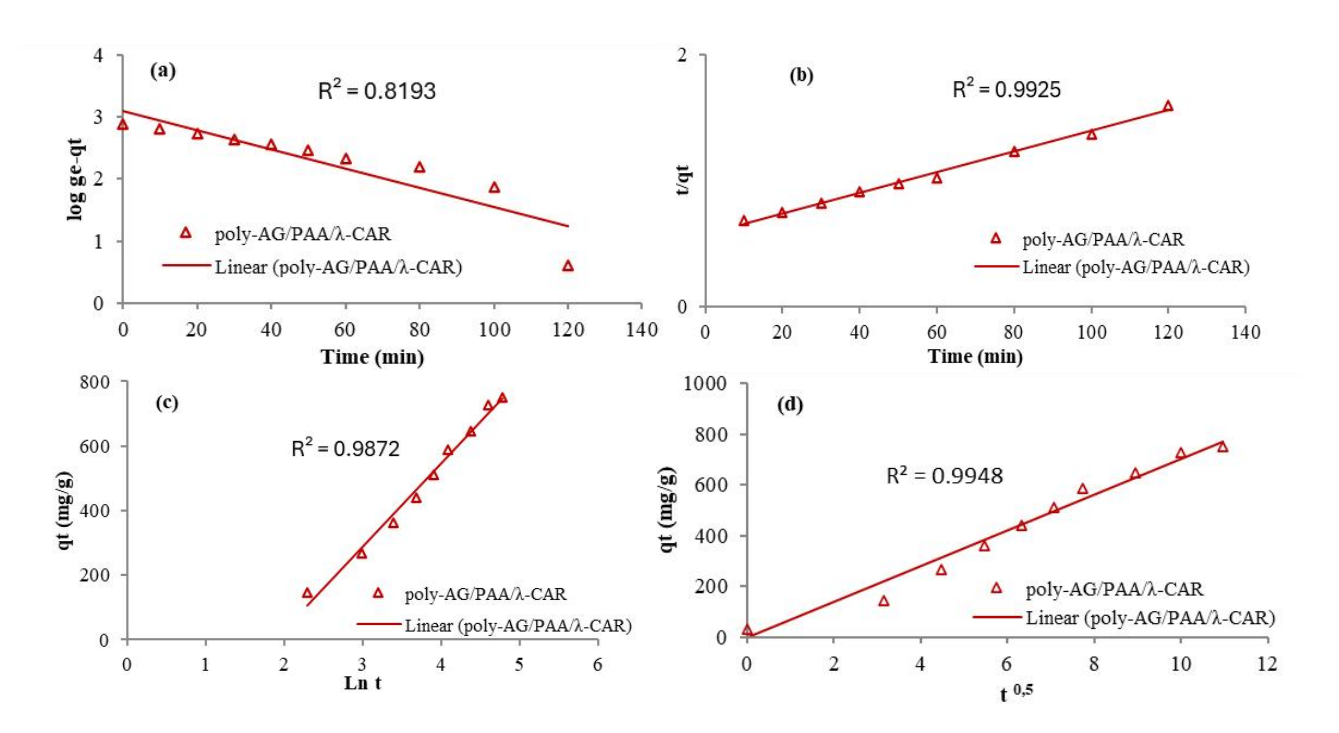


Figure 8. Fitted kinetic curves based on: (a) pseudo-first-order, (b) pseudo-second-order, (c) Elovich, and (d) intraparticle diffusion models

Table 1. Overview of kinetic parameters for the poly-AG/PAA/λ-CAR biosorbent composite

Equations	Parameters	poly-AG/PAA/λ-CAR		
	K1 (1/min)	0.0188		
Pseudo first order	$q_e(mg/g)$	828.7		
	\mathbb{R}^2	0.819		
Pseudo second Order	K ₂	0.000019		
	q	713.7		
	h	17.24		
	\mathbb{R}^2	0.992		
Elovich	α (mg/g/min)	0.0038		
	β (mg/g/min)	0.0042		
	\mathbb{R}^2	0.982		
Industrial 1 and 1 CC at an	$K_1 \left(mgg^{-1} \cdot min^{1/2} \right)$	70.319		
Intra-particular- diffusion	\mathbb{R}^2	0.994		

3.3. Adsorption Isotherm Study

The adsorption behavior of Rhodamine B (RhB) onto the poly-AG/PAA/ λ -CAR biosorbent composite was evaluated using Langmuir, Freundlich, and Temkin isotherm models, and the corresponding parameters are summarized in Table 2. For the Langmuir sotherm results in Figure 9a show a maximum adsorption capacity (qL) remained constant at 1111.1 mg/g across all temperatures, indicating a high potential for monolayer adsorption. The Langmuir constant (KL) decreased significantly from 0.642 at 22 °C to 0.0096 at 60 °C, suggesting that adsorption affinity diminishes with increasing temperature. The high correlation coefficients ($R^2 = 0.961$ -0.991) confirm that the Langmuir model accurately describes the adsorption process, implying that adsorption occurs predominantly on homogeneous sites forming a monolayer [40].

Freundlich Isotherm's results in Figure 9-b reveals the decrease of Freundlich constant (KF) and adsorption intensity (nF) with temperature, from 3.12 and 2.506 at 22°C to 1.85 and 1.328 at 60°C, respectively. This indicates that the adsorption is more favorable at lower temperatures and that surface heterogeneity plays a role in the adsorption process. The R2 values (0.853-0.952) suggest a moderate fit, confirming that the surface of the biosorbent is not completely uniform.

Temkin constants (B_T and A_T) in Figure 9-c indicate moderate adsorption energies, consistent with physical adsorption mechanisms such as electrostatic interactions or hydrogen bonding. The correlation coefficients (R² = 0.971-0.987) demonstrate that the Temkin model also describes the adsorption behavior effectively [41,42].

The adsorption of RhB onto poly-AG/PAA/λ-CAR is predominantly monolayer and exothermic, with higher adsorption efficiency at lower temperatures. The Langmuir model provides the best fit, while Freundlich and Temkin analyses indicate moderate surface heterogeneity and interaction energies, respectively. These results highlight the potential of this composite as a highly efficient biosorbent for dye removal from aqueous solutions.

The thermodynamic analysis shows that adsorption of Rhodamine B onto the poly-AG/PAA/λ-CAR composite is spontaneous and exothermic. The average enthalpy change, $\Delta H^{\circ} = -13.6 \text{ Kj.mol}^{-1}$ indicates the process releases heat. The negative entropy change, $\Delta S^{\circ} = -30.5 \text{ J.mol}^{-1} \text{K}^{-1}$, reflects decreased randomness at the solid-solution interface on dye uptake, consistent with dye molecules becoming more ordered when bound to the polymer. The Gibbs free energy values ($\Delta G^{\circ}_{.295K} = -4.6 \text{ kJ.mol}^{-1}$, $\Delta G^{\circ}_{313K} = -4.07 \text{ kJ.mol}^{-1}$ and $\Delta G^{\circ}_{333K} = -3.46 \text{ kJ.mol}^{-1}$) are negative at all measured temperatures but become less negative as temperature increases, showing that adsorption is thermodynamically less favorable at higher temperature, again consistent with an exothermic process.

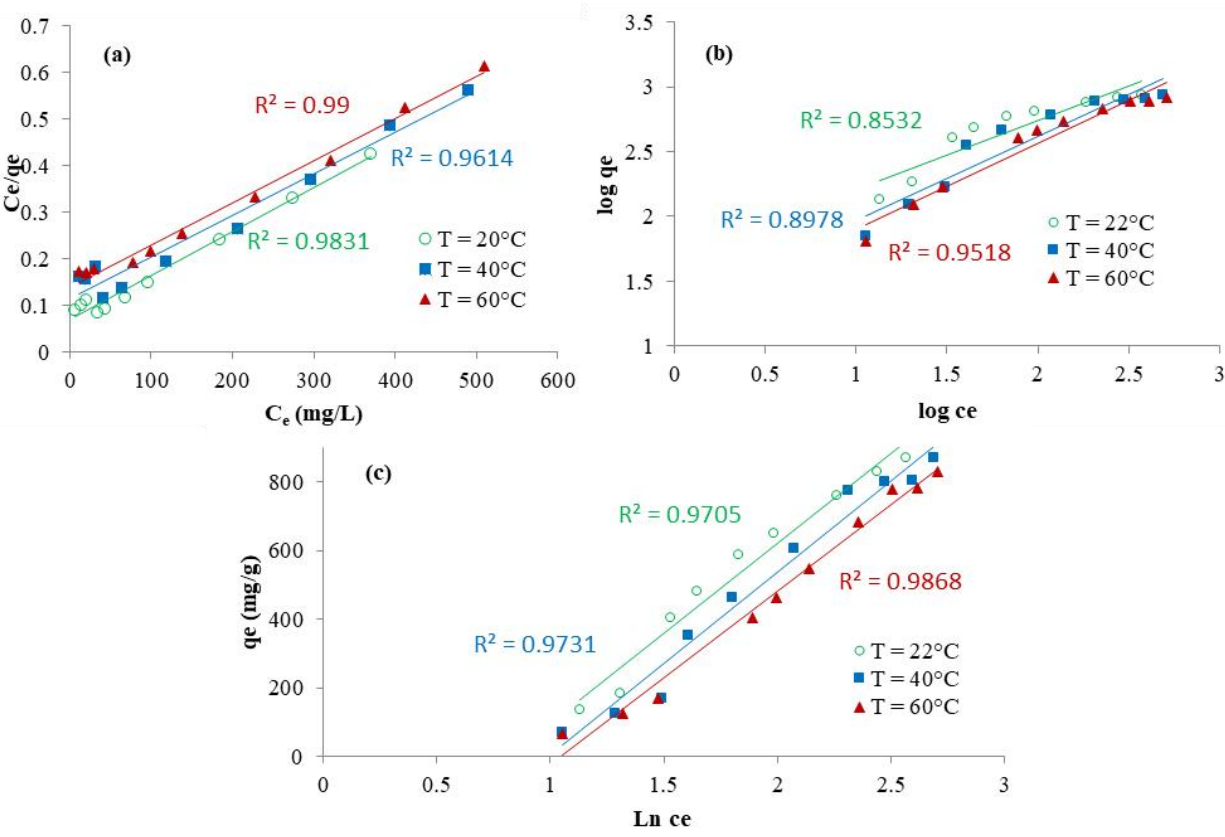


Figure 9. Adsorption equilibrium data fitted to: (a) Langmuir, (b) Freundlich, and (c) Temkin models.

Table 2. Adsorption isotherm data for RhB onto poly-AG/PAA/λ-CAR composite fitted using Langmuir, Freundlich, and Temkin models.

T (°C)	Langmuir		Freundlich			Temkin			
	K _L	$q_{\rm L}$	R ²	K_{F}	n_{F}	R ²	B_T	A_T	R ²
22	0.642	1111.1	0.983	3,12	2.506	0.853	0.818	2.267	0.971
40	0.016	1111.1	0.961	2.05	1.603	0.898	0.992	2.699	0.973
60	0.0096	1111.1	0.991	1.85	1.328	0.952	1.045	2.843	0.987

Conclusion

A novel ternary composite adsorbent, poly-AG/PAA/ λ -CAR, was successfully synthesized and demonstrated exceptional efficiency in removing Rhodamine B (RhB) from aqueous media. Comprehensive characterization confirmed the formation of a robust and functionalized network: FTIR analysis verified successful crosslinking and the presence of key functional groups; swelling studies showed that the crosslinked matrix exhibited over twice the swelling capacity of the uncrosslinked polymers, reflecting superior hydrophilicity derived from the synergistic contribution of alginate and λ -carrageenan reinforced by poly(acrylic acid) (PAA); SEM micrographs revealed a highly porous and rough surface with an interconnected morphology exposing abundant hydroxyl, carboxyl, ester, and sulfate sites crucial for dye binding.

Batch adsorption experiments indicated rapid equilibrium within 60 minutes and maximum performance at pH 8. Kinetic modeling confirmed that adsorption followed the pseudo-second-order model with an excellent fit ($R^2 > 0.99$), consistent with a chemisorption-driven process involving electron sharing and ion-exchange interactions between the dye molecules and the functional groups of the composite. The Langmuir model yielded a remarkable maximum adsorption capacity of 1111.1 mg g⁻¹, while the Freundlich and Temkin models revealed surface heterogeneity and moderate adsorbate—adsorbent interactions. Thermodynamic analysis indicated an exothermic and spontaneous process, suggesting that strong electrostatic and hydrogenbonding interactions contribute to dye uptake and are favored at lower temperatures.

Furthermore, reusability tests demonstrated that the composite maintained about 85% of its original capacity after five adsorption—desorption cycles, confirming its excellent structural stability and regeneration potential. These findings highlight the synergistic effects of the three polymeric components, combining chemical functionality, high porosity, and mechanical resilience.

In summary, the poly-AG/PAA/ λ -CAR composite exhibits high adsorption capacity, stability, and reusability, establishing it as a sustainable and promising biosorbent for industrial wastewater treatment. Future studies will extend its application to real effluents to evaluate performance under complex environmental conditions.

Funding: The authors gratefully acknowledge Qassim University, represented by the Deanship of Graduate Studies and Scientific Research, on the financial support for this research under the number (QU-J-PG-2-2025-56675) during the academic year 1446 AH / 2024 AD.

Conflicts of Interest: The authors declare no conflict of interest.

References

- 1. Pearce, C. I., Lloyd, J. R., Guthrie, J. T. (2003). The removal of colour from textile wastewater using whole bacterial cells: A review. Dyes and Pigments, 58(3), 179–196. DOI 10.1016/S0143-7208(03)00064-0.
- 2. Gupta, V. K., Suhas. (2009). Application of low-cost adsorbents for dye removal—A review. Journal of Environmental Management, 90(8), 2313–2342. DOI 10.1016/j.jenvman.2008.11.017.
- 3. Zheng, T., Holford, T. R., Mayne, S. T., Owens, P. H., Boyle, P. et al. (2002). Use of hair colouring products and breast cancer risk: A case-control study in Connecticut. European Journal of Cancer, 38(12), 1647–1652. DOI 10.1016/S0959-8049(02)00138-7.
- 4. Crini, G. (2006). Non-conventional low-cost adsorbents for dye removal: A review. Bioresource Technology, 97(9), 1061–1085. DOI 10.1016/j.biortech.2005.05.001.5. Nafea, E.-S. and A.M. Younis, Bioremoval of phenol from aqueous solution using Sea weed Sargassum muticum (Yendo) Fensholt. Aquatic Science and Fish Resources (ASFR), 2020. 1: p. 11-16.
- 5. Myung, H.H., et al. Chemical Precipitation Treatment for the Disperse Dyes Removal. Textile Coloration and Finishing, 2002. 14(2): p. 40-50.
- 6. Naim, M.M.; Al-harby, N.F.; El Batouti, M.; Elewa, M.M. Macro-Reticular Ion Exchange Resins for Recovery of Direct Dyes from Spent Dyeing and Soaping Liquors. *Molecules* **2022**, *27*, 1593.
- 7. Abdelhamid, A.E., Elsayed, A.E., Naguib, M. et al. Effective Dye Removal by Acrylic-Based Membrane Constructed from Textile Fibers Waste. Fibers Polym 24, 2391–2399 (2023).
- 8. Wang, L.K., et al., Physicochemical treatment consisting of chemical coagulation, precipitation, sedimentation, and flotation. Integrated natural resources research, 2021: p. 265-397.
- 9. Amini, A., et al., Environmental and economic sustainability of ion exchange drinking water treatment for organics removal. Journal of Cleaner Production, 2015. 104: p. 413-421.
- 10. Liu, C., et al., Evaluating the efficiency of nanofiltration and reverse osmosis membrane processes for the removal of perand polyfluoroalkyl substances from water: A critical review. Separation and Purification Technology, 2022. 302: p. 122161.
- 11. Wang, T. et al. Mechanistic insights into adsorption-desorption of PFOA on biochars: effects of biomass feedstock and pyrolysis temperature, and implication of desorption hysteresis Sci. Total Environ. 2024. P: 177668.
- 12. Liu, Y. et al. Effect of morphology on adsorption kinetics of magnesium oxide for the removal of methyl orange Desalin. Water Treat. 2017. 98: p. 326-335
- 13. Ibrahim, M.A. et al. Influence of size and surface charge on the adsorption behaviour of silicon dioxide nanoparticles on sand particles Colloids Surf. A: Physicochem. Eng. Asp. 2023. **674**: p. 131943.
- 14. Alminderej, F.M.; Ammar, C.; El-Ghoul, Y. Functionalization, characterization and microbiological performance of new biocompatible cellulosic dressing grafted chitosan and Suaeda fruticosa polysaccharide extract. *Cellulose* **2021**, *28*, 9821–9835.

- 15. Alminderej, F.M.; El-Ghoul, Y. Synthesis and study of a new biopolymer-based chitosan/hematoxylin grafted to cotton wound dressings. Journal of Applied Polymer Science. 2019, 136, 47625.
- 16. Ammar, C., El-Ghoul, Y., & Jabli, M. (2021). Characterization and valuable use of Calotropis gigantea seedpods as a biosorbent of methylene blue. International Journal of Phytoremediation, 23(10), 1085-1094.
- 17. Chen, Y.; Sheng, Q.; Hong, Y.; Lan, M. Hydrophilic nanocomposite functionalized by carrageenan for the specific enrichment of glycopeptides. Anal. Chem. 2019, 91, 4047-4054.
- 18. EL-Ghoul, Y.; Alsamani, S. Highly Efficient Biosorption of Cationic Dyes via Biopolymeric Adsorbent-Material-Based Pectin Extract Polysaccharide and Carrageenan Grafted to Cellulosic Nonwoven Textile. Polymers 2024.
- 19. Alminderej, F.M., Ammar, C. & El-Ghoul, Y. Functionalization, characterization and microbiological performance of new biocompatible cellulosic dressing grafted chitosan and Suaeda fruticosa polysaccharide extract. Cellulose 28, 9821-9835 (2021).
- 20. Alsultan, R.M., El-Ghoul, Y. and Chiraz, A. Polysaccharide Chemical Functionalization: Innovative Advances, Techniques, Overview and Biological Applications. Egyptian Journal of Chemistry, 2025.
- 21. Joseph, T.M., et al., Chemical modifications of alginate-based biopolymers, in Handbook of Natural Polymers, Volume 2. 2024, Elsevier. p. 97-122.
- 22. Cao, Y., et al., Specific binding of trivalent metal ions to λ-carrageenan. International journal of biological macromolecules, 2018. 109: p. 350-356.
- 23. Al-Fakeh, M.S.; Alazmi, M.S.; EL-Ghoul, Y. Preparation and Characterization of Nano-Sized Co(II), Cu(II), Mn(II) and Ni(II) Coordination PAA/Alginate Biopolymers and Study of Their Biological and Anticancer Performance. Crystals 2023, 13,
- 24. Szewczuk-Karpisz, K., et al., Simultaneous adsorption of Cu (II) ions and poly (acrylic acid) on the hybrid carbon-mineral nanocomposites with metallic elements. Journal of Hazardous Materials, 2021. 412: p. 125138.
- 25. Chen, M., et al., Recent advances in alginate-based hydrogels for the adsorption-desorption of heavy metal ions from water: A review. Separation and Purification Technology, 2024: p. 128265.
- 26. Widarty, S. et al. The Efficiency of κ-Carrageenan-Chitosan-PVA-MWCNTs Membranes in Removing Methylene Blue, Rhodamine B, Bromocresol Purple, and Murexid from Water. Asean Journal of Chemical Engineering, 2023, 23, 282-289.
- 27. Kasaai, M.R. A review of several reported procedures to determine the degree of N-acetylation for chitin and chitosan using infrared spectroscopy. Carbohydr. Polym. 2008, 71, 497–508.
- 28. Rochas, C.; Lahaye, M.; Yaphe, W. Sulfate Content of Carrageenan and Agar Determined by Infrared Spectroscopy. Bot. Mar. 1986, 29, 335-340.
- 29. EL-Ghoul, Y.; Al-Fakeh, M.S.; Al-Subaie, N.S. Synthesis and Characterization of a New Alginate/Carrageenan Crosslinked Biopolymer and Study of the Antibacterial, Antioxidant, and Anticancer Performance of Its Mn(II), Fe(III), Ni(II), and Cu(II) Polymeric Complexes. Polymers 2023, 15, 2511.
- 30. Chen, Y.; Sheng, Q.; Hong, Y.; Lan, M. Hydrophilic nanocomposite functionalized by carrageenan for the specific enrichment of glycopeptides. Anal. Chem. 2019, 91, 4047-4054.
- 31. EL-Ghoul, Y.; Alsamani, S. Highly Efficient Biosorption of Cationic Dyes via Biopolymeric Adsorbent-Material-Based Pectin Extract Polysaccharide and Carrageenan Grafted to Cellulosic Nonwoven Textile. Polymers 2024.
- 32. EL-Ghoul, Y.; Ammar, C.; Alminderej, F.M.; Shafiquzzaman, M. Design and Evaluation of a New Natural Multi-Layered Biopolymeric Adsorbent System-Based Chitosan/Cellulosic Nonwoven Material for the Biosorption of Industrial Textile Effluents. Polymers 2021, 13, 322.
- 33. Ammar, C., El Ghoul, Y. and El Achari, A., 2015. Finishing of polypropylene fibers with cyclodextrins and polyacrylic acid as a crosslinking agent. Textile Research Journal, 85(2), pp.171-179.
- 34. Li, Y., Sun, S., Ma, M., Ouyang, Y., & Yan, W. (2008). Kinetic study and model of the photocatalytic degradation of rhodamine B (RhB) by a TiO2-coated activated carbon catalyst: Effects of initial RhB content, light intensity and TiO2 content in the catalyst. Chemical Engineering Journal, 142(2), 147-155.
- 35. Stanciu, M.-C.; Teacă, C.-A. Natural Polysaccharide-Based Hydrogels Used for Dye Removal. Gels 2024, 10, 243.
- 36. Kyzas, G. Z., Lazaridis, N. K., & Kostoglou, M. (2014). Adsorption/desorption of a dye by a chitosan derivative: experiments and phenomenological modeling. Chemical Engineering Journal, 248, 327-336.
- 37. Mazengarb, S.; Roberts, G.A.F. Studies on the diffusion of direct dyes in chitosan film. Prog. Chem. App. Chitin Derivat. 2009, 14, 25–32.
- 38. Gucek, A.; Sener, S.; Bilgen, S.; Mazmanci, A. Adsorption and kinetic studies of cationic and anionic dyes on pyrophyllite from aqueous solutions. J. Coll. Interf. Sci. 2005, 286, 53-60.
- 39. Ho, Y.S.; McKay, G. The kinetics of sorption of basic dyes from aqueous solution by sphagnum moss peat. Can. J. Chem. Eng. 1998, 76, 822-827.
- 40. Ammar, C.; Alminderej, F.M.; EL-Ghoul, Y.; Jabli, M.; Shafiquzzaman, M. Preparation and Characterization of a New Polymeric Multi-Layered Material Based K-Carrageenan and Alginate for Efficient Bio-Sorption of Methylene Blue Dye. Polymers 2021, 13, 411.
- 41. Agougui, H.; Sebeia, N.; Jabli, M. and El-Ghoul, Y.; Synthesis of hydroxyapatite-sodium metasilicate via double decomposition method: Characterization and application to the removal of methylene blue. Inorganic Chemistry Communications 2021, 133, 108986.
- 42. Ngulube, T.; Gumbo, J.R.; Masindi, V.; Maity, A. Calcined magnesite as an adsorbent for cationic and anionic dyes: Characterization, adsorption parameters, isotherms and kinetics study. Heliyon 2018, 4, 838.